BIOCHEMICAL PHARMACOLOGY 76 (2008) 707–716

available at www.sciencedirect.com

ScienceDirect

journal homepage: www.elsevier.com/locate/biochempharm

Interference with actin dynamics is superior to disturbance of microtubule function in the inhibition of human ovarian cancer cell motility

Marcel N.A. Bijman [a], *Maria P.A. van Berkel* [a], *Geerten P. van Nieuw Amerongen* [b], *Epie Boven* [a,*]

[a] *Department of Medical Oncology, VU University Medical Center, De Boelelaan 1117, 1081 HV Amsterdam, The Netherlands*
[b] *Department of Physiology, VU University Medical Center, Amsterdam, The Netherlands*

ARTICLE INFO

Article history:
Received 2 May 2008
Accepted 17 June 2008

Keywords:
Ovarian cancer
Cytoskeleton
Motility
Microtubule-targeting agents
F-actin

ABSTRACT

Cellular movement is mainly orchestrated by the actin and microtubule cytoskeleton in which Rho GTPases closely collaborate. We studied whether cytoskeleton-interfering agents at subtoxic and 50% growth-inhibiting concentrations affect motility of five unselected human ovarian cancer cell lines. Cisplatin and doxorubicin as control cytotoxic agents were not effective, the microtubule-targeting agents docetaxel, epothilone B and vinblastine only marginally inhibited cell motility, while the actin-targeting agent cytochalasin D was most potent in hampering both cell migration and invasion. Disturbance of microtubule dynamics by docetaxel did not importantly affect the cellular structures of β-tubulin and F-actin. In contrast, hindrance of actin dynamics by cytochalasin D resulted in loss of lamellipodial extensions, induced thick layers of F-actin and disorder in cellular organization. In OVCAR-3 cells the activity of Rac1 was only slightly diminished by docetaxel, but clearly reduced by cytochalasin D. In conclusion, targeting the actin cytoskeleton might provide a means to prevent metastasis formation.

1. Introduction

Ovarian cancer is the fifth leading cause of cancer death in the western world. The lethality of ovarian cancer is mainly due to the fact that more than 70% of patients show distant metastases at the time of diagnosis. Treatment of ovarian cancer consists of optimal debulking surgery combined with platinum–taxane combination chemotherapy. Survival in advanced ovarian cancer largely depends on the size of residual tumor lesions [1]. The metastatic potential of ovarian cancer cells is unique as compared to other tumor types: at early stage the tumor cells reside in an intact ovary, but at later stages the ovary disrupts which enables tumor cells to invade directly into the peritoneal lining of the abdominal cavity or to spread through the lymphatics that drain the ovaries [2]. Understanding the molecular mechanism of ovarian cancer cell motility might facilitate the development of possible inhibitors of migration and invasion as a novel approach for treatment.

Cellular movement is orchestrated by microtubules and the actin cytoskeleton. Together they provide cell shape and maintain cellular structure and polarization. Actin provides the driving force during the process of cell migration via the formation of contractile bundles (stress-fibers) through the cell body and the creation of lamellipodia at the leading edge. Microtubules support movement by filling in cellular extensions, and activating molecules that provide positive feedback in the motility process [3,4]. These activating molecules

* *Corresponding author*. Tel.: +31 20 4444336; fax: +31 20 4444079.
E-mail address: e.boven@vumc.nl (E. Boven).
0006-2952/$ – see front matter
doi:10.1016/j.bcp.2008.06.014

include members of the Rho GTPase family. Detailed analysis of how Rho GTPases work in cells is very complex. Most knowledge of their role as regulators of cytoskeleton dynamics has been acquired from members Cdc42, Rac1 and RhoA [5–7]. Cdc42 mediates polarity of the cell, enabling motility to be initiated and propagated in the desired direction [8]. Rac1 induces the development of cellular extensions (lamellipodia) at the leading edge, actin polymerization and formation of new adhesion sites to the matrix [5,6]. RhoA mediates assembly and contraction of actin–myosin filaments in the cell body and at the rear, resulting in forward movement [5,6]. Interference with actin or microtubule dynamics by cytoskeleton-targeting anticancer agents will result in decreased cell motility.

Standard cytotoxic agents that target the cytoskeleton are mainly used to interfere with the mitotic machinery leading to tumor cell death. Earlier, we have shown in endothelial cells that subtoxic concentrations of microtubule-targeting agents that do not affect cell proliferation can already inhibit migration and invasion [9]. We hypothesized that low concentrations of these compounds might interfere with motility of tumor cells as well. Earlier, it has been suggested that the actin cytoskeleton may also be a target for cancer treatment [10]. Metronomic therapy directed towards microtubule and actin filament polymerization dynamics might be a useful approach to inhibit cell kinetics and, as a result, metastasis formation.

This study aims to provide insight into the capacity of microtubule- and actin-interfering agents to inhibit human ovarian cancer cell motility. We selected representatives of four classes of cytoskeleton-targeting agents: taxanes, epothilones, Vinca alkaloids and cytochalasins. Taxanes stabilize microtubules, whereby the dynamic reorganization and depolymerization are inhibited. Epothilones are structurally unrelated to taxanes, but share their ability to stabilize microtubules [11]. Vinca alkaloids also affect microtubule integrity, but display a different mode of action than taxanes and epothilones; they inhibit tubulin polymerization and formation of the mitotic spindle. Whereas docetaxel, epothilone B and vinblastine interfere with microtubule function, cytochalasin D inhibits F-actin polymerization. It will reduce actin filament mass and stabilizes the barbed end dynamics of the filaments [10,12]. Cisplatin and doxorubicin were included as standard cytotoxic agents that do not target the cytoskeleton. The drug concentrations used were subtoxic and 50% growth-inhibiting concentrations as well as equitoxic to be able to compare the potency of the different compounds. In addition, the interference with microtubule or actin function associated with the integrity of the cytoskeleton was studied concurrently with possible changes in the activities of Rac1 and Cdc42.

2. Materials and methods

2.1. Cell culture

Five human ovarian cancer cell lines were used: A2780, H134, OVCAR-3, IGROV-1 and SKOV-3 [13,14]. The cells were grown in tissue culture flasks in Dulbecco's modified Eagle's medium (DMEM; Invitrogen, Breda, the Netherlands) supplemented with 10% fetal calf serum (FCS, Invitrogen), 100 U/ml penicillin and 100 μg/ml streptomycin (Bio-Whittaker, Verviers, Belgium) at 37 °C in 5% CO_2.

2.2. In vitro antiproliferative assay

The antiproliferative effects of cisplatin (Bristol-Myers Squibb, Woerden, the Netherlands), doxorubicin (Pharmachemie, Haarlem, the Netherlands), docetaxel (sanofi aventis, Antony, France), epothilone B (Novartis, Arnhem, the Netherlands), vinblastine (Eli-Lilly, Houten, the Netherlands) and cytochalasin D (Sigma–Aldrich, Zwijndrecht, the Netherlands) were analyzed in the MTT assay. Molar stock solutions were further diluted in culture medium immediately before use. Cells were plated in culture medium in 96-well plates at 3000 cells per well in quadruplicate and were exposed to a drug concentration range for 1 h. After washing, cells were grown in culture medium for an additional 96-h period. The number of viable cells was determined by addition of 3-(4,5-dimethylthiazol-2-yl)-2,5-diphenyltetrazoliumbromide (MTT; Sigma–Aldrich). The extinction of the formazan product after conversion of MTT by mitochondria of metabolically active cells was measured at 540 nm on a multiscan plate reader (Thermo Biosciences, Breda, the Netherlands). Results were expressed in IC50 and IC10 values, being the drug concentrations responsible for 50% and 10% growth inhibition, respectively, as compared to control cell growth. Both the IC50 and the IC10 concentrations were used in further experiments. The IC10, the highest non-toxic concentration (HNTC) of a drug, was checked in parallel MTT assays.

2.3. Migration assay

Ovarian cancer cells were seeded in duplicate in wells of a 24-well plate and grown to confluence. The cells were treated with drugs (HNTC, IC50) for 1 h followed by replacement by culture medium. With a sterile pipette tip a wound was applied in two perpendicular directions in the confluent cell layer. Immediately after wounding and at time-point 12 h wounds were captured at 25× magnification by using a confocal laserscan microscope (TCS 4D; Leica, Jena, Germany) and Q500MC software (Leica). At time-point 12 h wound width was measured in four areas and expressed as a percentage of the wound width at time-point 0 h.

2.4. Invasion assay

Ovarian cancer cell invasion was measured in a 24-well plate transwell system (Falcon, Woerden, the Netherlands) containing inserts with a fluorescence-blocking filter and a pore size of 8 μm (HTS fluoroblock; Falcon). The inserts were coated on the bottom with 2 μg/ml fibronectin (ICN, Zoetermeer, the Netherlands), washed with phosphate-buffered saline (PBS; Bio-Whittaker) and coated on the upper side with 5 μg extracellular matrix gel (ECM gel/Matrigel; Sigma–Aldrich) in 100 μl PBS. A number of 2×10^5 tumor cells were seeded on top of the ECM gel layer in each well in duplicate and were allowed to settle for 4 h. Thereafter, cells were exposed to drugs (HNTC, IC50) for 1 h, or were left untreated (control) followed by

replacement by culture medium containing 1% FCS in the upper compartment. Culture medium containing 10% FCS was added to the lower compartment of the system to elicit tumor cell invasion through the ECM gel layer. The cells were allowed to invade for 48 h. Thirty minutes prior to analysis, 5 μM calcein-AM (Molecular Probes, Leiden, the Netherlands) was added to the lower compartment, a substance that will be intracellularly converted to the polar fluorochrome calcein, including by cells still attached to the bottom of the filter. Calcein fluorescence in the lower compartment was measured in a spectrafluor multiplate reader (Tecan, Gorinchem, the Netherlands) at λ^{exc} = 492 nm and λ^{em} = 535 nm.

2.5. Immunocytochemistry

Ovarian cancer cells were seeded and grown to confluence on glass coverslips in a 24-well plate. Cells were then treated or not with drugs (IC50) for 1 h. A wound was formed in the confluent cell layer by a gentle scrape with a sterile pipette tip. Cells were washed with medium and culture medium was added for an 8-h period after which cells were fixed with 3.7% formaldehyde without prior PBS-washing steps in order to preserve cytoskeletal integrity. Fixed cells were made permeable with 0.2% Triton X-100 (Sigma–Aldrich) in PBS and incubated with a monoclonal antibody against β-tubulin (1:50; Molecular Probes) for 2 h in 3% bovine serum albumin (BSA; ICN) in PBS. After washing, cells were incubated with Hoechst 33342 (1:500; Sigma–Aldrich) for nuclear staining and rhodamine-conjugated phalloidin (1:200; Molecular Probes) for F-actin staining. A secondary FITC-labeled mouse-IgG targeting antibody (1:120; DAKO, Amsterdam, the Netherlands) was used to visualize β-tubulin. After three washing steps of 15 min, coverslips were mounted in Vecta Shield (Vector Laboratories, Burlingame, CA) and digital imaging was performed on a Zeiss Axiovert 200 Marianas™ inverted microscope (Zeiss, Leusden, the Netherlands). Images were captured by a digital camera (Sensicam, Cooke, Tonawanda, NY) through a 10× and 40× air lens and analyzed by Slidebook™ software (Version 4.0; Intelligent Imaging Innovations, Denver, CO).

2.6. Rac1/Cdc42 activity assay

Ovarian cancer cells were grown to 80% confluence in 10 cm petri-dishes and rendered quiescent in culture medium with 1% FCS overnight. Rac1/Cdc42 activation was provoked by addition of complete culture medium (10% FCS), while at the same time drugs (IC50) were added or not. One hour thereafter, Rac1/Cdc42 activity was analyzed using the Rac1/Cdc42 Activation Assay Kit (Chemicon, Chandlers Ford, United Kingdom) according to instructions provided by the manufacturers. Briefly, after washing cells were lysed in assay buffer (supplemented with 0.5 mM trypsin inhibitor, 0.5 μg/ml leupeptin, 1 mM PMSF) and centrifuged to remove cell debris. To determine total Rac1/Cdc42 levels, 40 μl of each sample was stored at −80 °C for separate analysis. The remaining 960 μl of the supernatant was incubated with 10 μg of agarose-conjugated p21-binding domain of PAK-1, which binds both activated Rac1 and Cdc42, for 1 h at 4 °C while tumbling. Agarose beads with bound active Rac1/Cdc42 were washed four times in assay buffer, resuspended in 30 μl SDS-sample buffer (10% glycerol, 3% SDS, 20 μg/ml bromophenol blue, 25 μg/ml β-mercaptoethanol, 0.6 M Tris, pH 6.7) and boiled for 10 min.

Active (GTP-bound) and total Rac1/Cdc42 protein levels in each sample were analyzed by Western blot. Samples obtained from the Rac1/Cdc42 activity assay were subjected to 12% polyacrylamide gel electrophoresis (75 V, 30 min followed by 125 V, 1 h). The separated proteins were transferred to a polyvinylidene fluoride membrane (PVDF; Millipore, Etten-Leur, the Netherlands) by electrotransfer (400 mA, 2 h). The blots were blocked with 10% milk (Protifar; Nutricia, Zoetermeer, the Netherlands) in Tris-buffered saline–Tween 20 (TBS–T: 10 mM Tris, pH 8.0, 150 mM NaCl, 0.0025% Tween 20) at room temperature for 1 h and incubated overnight at 4 °C with the Kit-provided mouse monoclonal antibody against Rac1 (1:500; Chemicon) diluted in 5% BSA/TBS–T. After the membrane was washed three times for 5 min with TBS–T it was incubated with 5% milk/TBS–T, containing horseradish peroxidase (HRP)-linked anti-mouse-IgG secondary antibody, for 1 h at room temperature. After three TBS–T washing steps of 15 min Rac1 protein was visualized by enhanced chemoluminescence. Cdc42 protein was visualized on the same blot. To that end, the Rac1 blot was stripped for 15 min in strip buffer (Pierce, Rockford, IL) and washed three times with TBS–T. Subsequently, the blots were blocked again with 10% milk in TBS–T for 1 h, incubated overnight with the Kit-provided mouse monoclonal antibody directed against Cdc42 (1:250; Chemicon) and thereafter, incubated with HRP-linked anti-mouse-IgG secondary antibody for 1 h. Proteins were visualized on photography film (Pharmacia, Uppsala, Sweden) by enhanced chemoluminescence.

2.7. Statistics

The effects of the agents on cellular migration and invasion were subjected to statistical analysis by one-way ANOVA followed by the Bonferroni adjustment, using SPSS software (SPSS Inc., Chicago, IL). The level of significance was set at $p < 0.05$.

3. Results

3.1. Determination of highest non-toxic drug concentrations and IC50 values in ovarian cancer cell lines

The antiproliferative effects of cisplatin, doxorubicin, docetaxel, epothilone B, vinblastine and cytochalasin D in a panel of ovarian cancer cell lines were determined by the MTT assay and expressed as HNTC and IC50. Cells were exposed to the drugs for 1 h, followed by a 96-h drug-free period. Table 1 shows HNTCs (fixed concentrations, first column) and the mean percentage of cell growth when cells were exposed to HNTCs (second column). Table 2 depicts the mean IC50 values of the drugs in the different cell lines. Epothilone B was most potent and inhibited 50% of ovarian cancer cell growth at a concentration varying between 0.8 and 5.0 nM. Cisplatin was least potent and concentrations varying between 8 and 50 μM were required to achieve a 50% growth-inhibiting effect.

Table 1 – Antiproliferative effects of highest non-toxic concentrations (HNTC) of cytotoxic agents in ovarian cancer cell lines after a 1-h drug exposure period followed by a 96-h drug-free period

HNTC[a]	A2780		H134		OVCAR-3		IGROV-1		SKOV-3	
	HNTC	Growth[b]	HNTC	Growth[b]	HNTC	Growth[b]	HNTC	Growth[b]	HNTC	Growth[b]
Cisplatin (μM)	6.3	94.9 ± 7.2	6.3	95.9 ± 9.8	1.7	92.2 ± 4.4	1.0	96.6 ± 7.3	7.6	101.0 ± 5.4
Doxorubicin (nM)	9.8	93.6 ± 2.5	39.0	100.4 ± 2.2	48.8	97.6 ± 4.2	175.0	91.2 ± 4.5	21.7	102.4 ± 6.4
Docetaxel (nM)	1.0	98.3 ± 8.5	3.9	104.2 ± 9.3	6.2	95.5 ± 3.5	2.4	93.1 ± 5.4	0.8	98.4 ± 7.5
Epothilone B (pM)	61.0	98.4 ± 2.4	61.0	105.9 ± 11.5	549.0	97.7 ± 3.5	233.0	89.9 ± 11.6	595.0	98.5 ± 4.1
Vinblastine (nM)	1.0	100.7 ± 4.4	3.9	100.9 ± 5.2	2.2	96.6 ± 4.4	6.9	100.7 ± 7.1	2.0	94.2 ± 9.2
Cytochalasin D (μM)	0.6	98.6 ± 1.0	0.6	91.2 ± 5.5	1.1	93.1 ± 7.2	0.5	92.1 ± 7.3	0.2	95.9 ± 7.8

[a] Highest non-toxic concentration, concentration of the drug not yet interfering with proliferation.
[b] Cell growth at HNTC expressed as a percentage of control cell growth; mean ± S.D. of at least three separate experiments.

Table 2 – IC50 values of cytotoxic agents in ovarian cancer cell lines after a 1-h drug exposure followed by a 96-h drug-free period

IC50[a]	A2780	H134	OVCAR-3	IGROV-1	SKOV-3
Cisplatin (μM)	23.4 ± 16.5	27.9 ± 25.0	25.9 ± 15.9	7.7 ± 2.3	49.6 ± 14.8
Doxorubicin (nM)	67.7 ± 15.3	1080.1 ± 129.9	326.0 ± 100.6	220.0 ± 65.3	301.2 ± 84.2
Docetaxel (nM)	8.7 ± 3.1	49.3 ± 11.7	23.8 ± 5.27	7.8 ± 5.2	6.4 ± 2.5
Epothilone B (nM)	1.2 ± 1.2	3.4 ± 7.1	5.0 ± 2.0	0.8 ± 0.3	1.4 ± 1.3
Vinblastine (nM)	7.5 ± 1.9	21.6 ± 8.4	10.9 ± 5.4	26.10 ± 25.6	4.2 ± 3.8
Cytochalasin D (μM)	3.0 ± 0.9	3.7 ± 10.8	8.5 ± 3.1	3.2 ± 1.2	3.6 ± 1.2

[a] Drug concentration resulting in 50% growth inhibition as compared to control cell growth; mean ± S.D. of at least three separate experiments.

3.2. *Ovarian cancer cell migration is affected by interference with the actin cytoskeleton*

The spontaneous migratory capacity of the five ovarian cancer cell lines is shown in Fig. 1. A2780 and H134 cells hardly moved during the 12 h of the experiment (mean values of 5.4% and 3.3% of wound closure, respectively). In contrast, OVCAR-3 and SKOV-3 rapidly filled the applied wound: after 12 h mean wound closure was 64.6% and 72.4% for OVCAR-3 and SKOV-3, respectively. IGROV-1 cells showed an intermediate rate of migration; a mean value of 17.7% was calculated after 12 h.

Because of their migratory potential, experiments on inhibition of motility by the cytoskeleton-targeting agents were conducted in OVCAR-3, SKOV-3 and IGROV-1 cells (Fig. 2). Upper and lower panels show wound closure as a ratio of control wound width (set at 1.00) at 12 h after a 1-h exposure to, respectively, HNTCs and IC50 of the six different compounds. HNTCs and IC50s of the cytotoxic agents cisplatin and doxorubicin did not affect the motility of the cancer cells. As for the microtubule-interfering agents, docetaxel and vinblastine inhibited IGROV-1 cell migration significantly at HNTC (mean ratios of 0.66 and 0.65, respectively; $p < 0.05$) and at IC50 (mean ratios of 0.60 and 0.40, respectively; $p < 0.01$), while epothilone B significantly hampered SKOV-3 migration at HNTC (mean ratio of 0.70; $p < 0.05$) and IC50 (mean ratio of 0.70; $p < 0.05$). The actin-interfering agent cytochalasin D inhibited migration most successfully at subtoxic concentrations (mean ratios of 0.24, 0.44 and 0.35 in IGROV-1, OVCAR-3 and SKOV-3, respectively; $p < 0.001$). Effects were further enhanced when 50% growth-inhibiting concentrations of the compound were applied: mean ratios of 0.11, 0.25 and 0.17 were calculated in, respectively, IGROV-1, OVCAR-3 and SKOV-3 cells ($p < 0.001$).

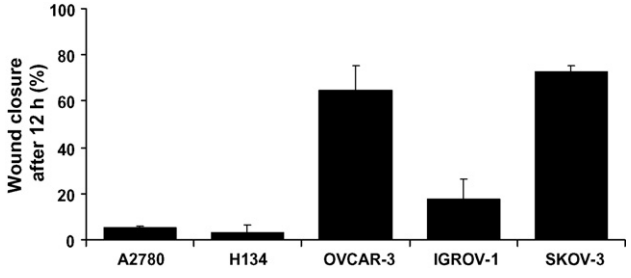

Fig. 1 – Migration assay. Ovarian cancer cells were seeded to confluence and a wound was applied in two perpendicular directions with a pipette tip. The cells were allowed to migrate for 12 h. Migratory capacity of the different cell lines is shown. Mean ± S.D. of at least three independent experiments.

3.3. *Ovarian cancer cell invasion is affected by interference with the actin cytoskeleton*

Ovarian cancer cell invasion was investigated in a transwell system. In the upper compartment of the system cells were seeded on top of a layer of artificial extracellular matrix (Matrigel). Cells were allowed to invade to the lower compartment for 48 h. Spontaneous invasive capacity was measured (medium containing 1% FCS in both the upper and lower compartment) and appeared to be most prominent for OVCAR-3 and SKOV-3 cells, while A2780, H134 and IGROV-1 hardly showed invasive cells (Fig. 3). When 10% FCS was added to the medium in the lower compartment invasion increased

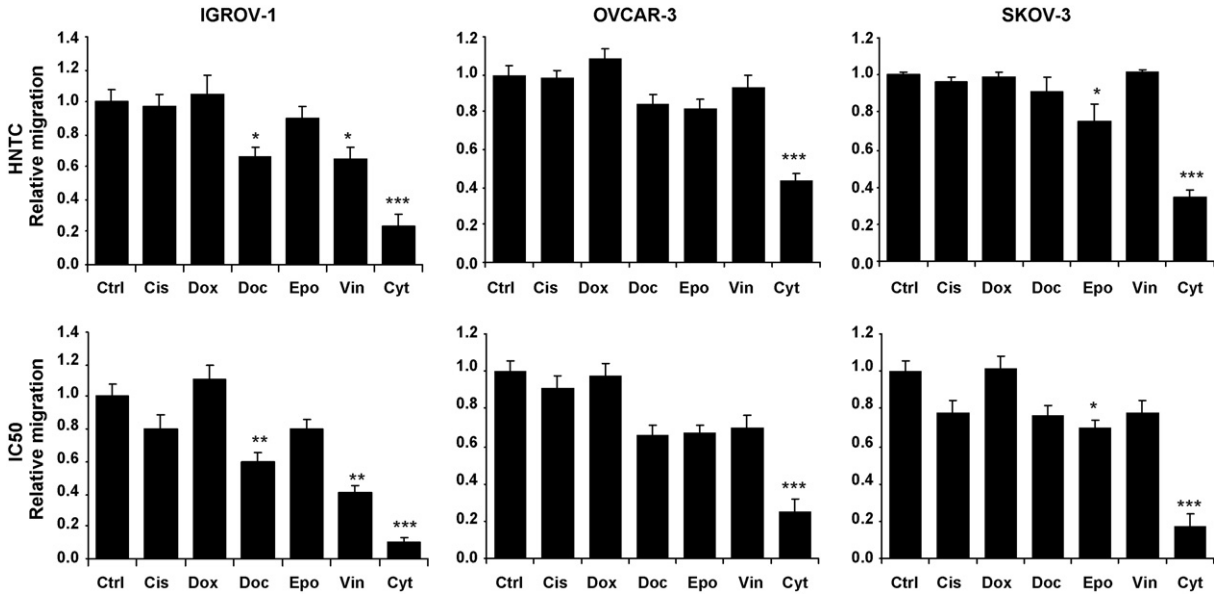

Fig. 2 – Migration assay. Upper panels: wound closure at 12 h of cells treated with the highest non-toxic concentrations (HNTC) as a ratio relative to control cell migration (set at 1.0). Lower panels: wound closure at 12 h of cells treated with 50% growth-inhibiting concentrations (IC50) of the indicated drugs. HNTC and IC50 values were as indicated in Tables 1 and 2. Mean migration ratios are given of at least three independent experiments, each with four distinct measurements of wound width in duplicate wounds. Ctrl, control; Cis, cisplatin; Dox, doxorubicin; Doc, docetaxel; Epo, epothilone B; Vin, vinblastine; Cyt, cytochalasin D. Bars, SEM; $^{*}p < 0.05$, $^{**}p < 0.01$, $^{***}p < 0.001$.

in most cell lines, but H134 still showed very modest invasion and A2780 did not invade at all. Based on these findings, OVCAR-3, SKOV-3 and IGROV-1 were chosen to study invasion after treatment with the cytoskeleton-interfering agents (Fig. 4).

Cisplatin and doxorubicin had no significant effect on ovarian cancer cell invasion at HNTC (Fig. 4, upper panel), but at IC50 (Fig. 4, lower panel) cisplatin slightly reduced IGROV-1

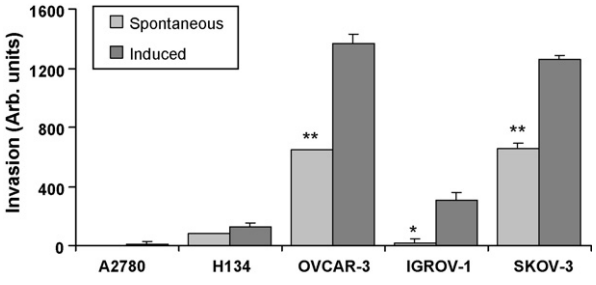

Fig. 3 – Invasion assay. Ovarian cancer cells were seeded in culture medium containing 1% FCS on top of a Matrigel layer (5 μg) in a transwell insert. Spontaneous invasion was measured in the lower compartment containing culture medium with only 1% FCS, whereas induction of invasion was measured by the addition of complete culture medium (10% FCS) to the lower compartment of the transwell system. The amount of liberated calcein from calcein-AM (5 μM) added to the lower compartment was measured after 48 h. Mean arbitrary units of calcein fluorescence are shown of at least three independent experiments. Bars, SEM; $^{*}p < 0.05$, $^{**}p < 0.005$.

and SKOV-3 invasion as compared to untreated cells (mean values of 74.5% and 75.1%, respectively). HNTCs of the microtubule-interfering agents had limited effects on invasion; docetaxel only slightly inhibited the invasion of IGROV-1 (mean value of 74.2%; n.s.) and SKOV-3 (mean value of 64.4%; $p < 0.05$), epothilone reduced IGROV-1 invasion (mean value of 48.5%; n.s.) and vinblastine had a minor anti-invasive effect on IGROV-1 and SKOV-3 (mean values of 76.3% and 74.1%, respectively; n.s.). The inhibitory capacity of the microtubule-interfering agents on invasion followed the same pattern when 50% growth-inhibiting concentrations were applied; reduction by docetaxel (mean value of 34.3%; $p < 0.05$), epothilone B (mean value of 21.1%; $p < 0.01$) and vinblastine (mean value of 35.4%; $p < 0.05$) was significant in IGROV-1, while in SKOV-3 invasion was significantly obstructed by docetaxel (mean value of 43.3%; $p < 0.001$). Of interest, cytochalasin D significantly prevented the invasion at HNTC in IGROV-1 (mean value of 37.5%; $p < 0.05$) and in all three cell lines at IC50; mean values at IC50 were calculated in IGROV-1 17.5% ($p < 0.01$), OVCAR-3 24.8% ($p < 0.001$) and SKOV-3 47.7% ($p < 0.005$).

3.4. *Interference with actin dynamics affects cytoskeletal integrity to a larger extent than disturbance of tubulin function*

The cytoskeletal changes in IGROV-1, OVCAR-3 and SKOV-3 morphology upon addition of docetaxel or cytochalasin D were examined after a 1-h drug exposure (IC50) and subsequent wounding of the cell monolayer. At 8 h after wounding images of the structures of the β-tubulin

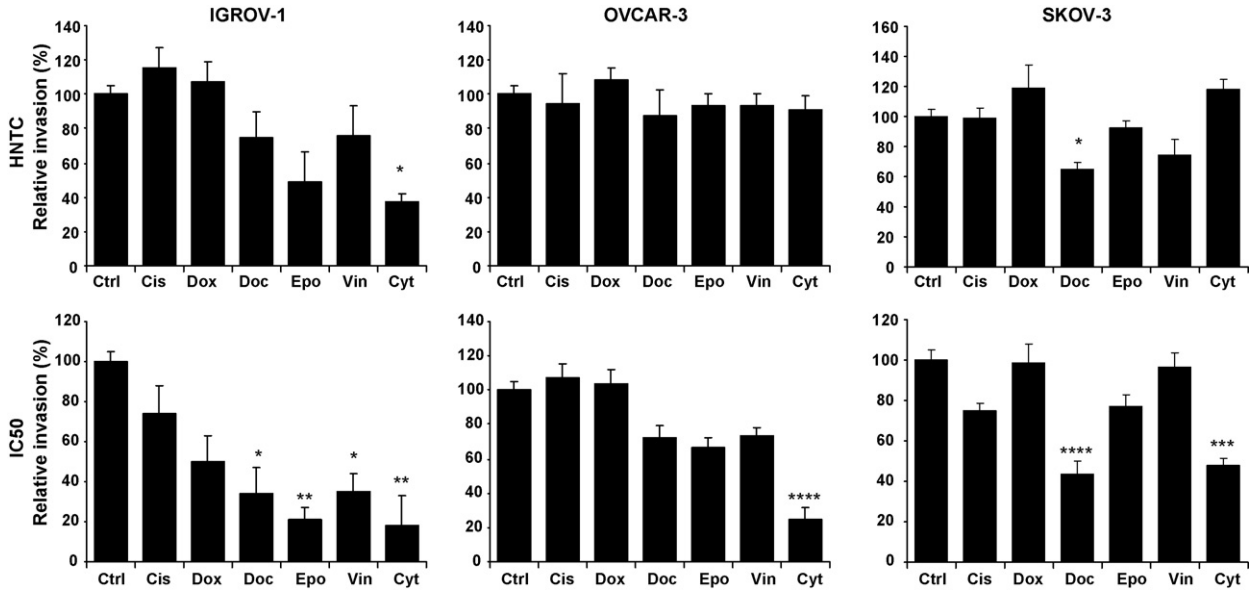

Fig. 4 – Invasion assay. Ovarian cancer cells were seeded on top of a Matrigel layer (5 μg) in a transwell insert. Invasion was induced by the presence of complete culture medium (10% FCS) in the lower compartment of the transwell system. Cells were treated with drugs for 1 h. Highest non-toxic concentrations (HNTC) and 50% growth-inhibiting concentrations (IC50) were as indicated in Tables 1 and 2. The number of invaded cells was assessed after 48 h by measuring the amount of liberated calcein from calcein-AM (5 μM) that was added to the lower compartment. Invasion towards 10% FCS by untreated cells was set at 100%. Mean percentages are shown of at least three independent experiments. Ctrl, control; Cis, cisplatin; Dox, doxorubicin; Doc, docetaxel; Epo, epothilone B; Vin, vinblastine; Cyt, cytochalasin D. Bars, SEM; $^{*}p < 0.05$, $^{**}p < 0.01$, $^{***}p < 0.005$, $^{****}p < 0.001$.

and F-actin cytoskeleton were captured by fluorescence microscopy (Fig. 5).

IGROV-1 cells are relatively small and show broad lamellipodia filled with microtubules in the direction of movement. Upon treatment with docetaxel or cytochalasin D cells were more compact. Lamellipodia were still visible after exposure to docetaxel, but tubulin was mostly present as a thick layer around the nucleus. Lamellipodia were ruffled by cytochalasin D and contained patchy layers of F-actin.

Untreated OVCAR-3 cells displayed broad F-actin extensions along the membrane at the leading edge in the direction of movement, which contained several radial F-actin spikes. Remarkably, these extensions were almost void of microtubules. Upon treatment with docetaxel only subtle changes in morphology were visible as compared to that of control cells; the intensity of the tubulin signal was slightly increased, but the F-actin extensions in the direction of movement remained present. Interference with actin dynamics by cytochalasin D resulted in pronounced changes in the cytoskeletal architecture in OVCAR-3 cells. F-actin extensions had mostly disappeared. Instead, a thick layer of F-actin contoured the cells and spike-like extensions of tubulin without actin support were visible.

A different pattern was visible in SKOV-3 control cells: broad F-actin lamellipodia at the leading edge in the direction of movement were filled with microtubules. Upon treatment with docetaxel subtle morphological changes were visible; microtubules formed a thick layer around the nucleus of some cells, but the F-actin extensions in the direction of movement remained present. In contrast, cytochalasin D treatment resulted in loss of the characteristic broad lamellipodia. Instead, the cells contained a thick layer of F-actin at the assumed leading edge and demonstrated a disorganized meshwork as a sign of complete disorder in orientation.

3.5. *Interference with actin dynamics inhibits Rac1 activity in OVCAR-3 cells*

Activity of both Rac1 and Cdc42 is tightly regulated by actin and tubulin dynamics; disturbances in the microtubule/actin integrity induced by docetaxel or cytochalasin D might result in a reduced functionality of these two key molecules in the onset of cell migration. OVCAR-3 cells were selected to pull down active Rac1 and Cdc42 from total cell lysates after a 1-h drug exposure (IC50). Levels were compared with total protein levels as assessed by Western blot (Fig. 6). Total levels of both Rac1 and Cdc42 remained the same in OVCAR-3 cells after treatment with either docetaxel or cytochalasin D. Interference with tubulin dynamics by docetaxel only slightly inhibited Rac1 activity, while Cdc42 activity remained unaffected. Interference with actin dynamics by cytochalasin D, however, resulted in potent inhibition of Rac1 activity, whereas Cdc42 activity was unaltered.

4. Discussion

At equitoxic drug doses we demonstrate that interference with actin dynamics is more effective in inhibiting human ovarian cancer cell motility than disturbance of microtubule function.

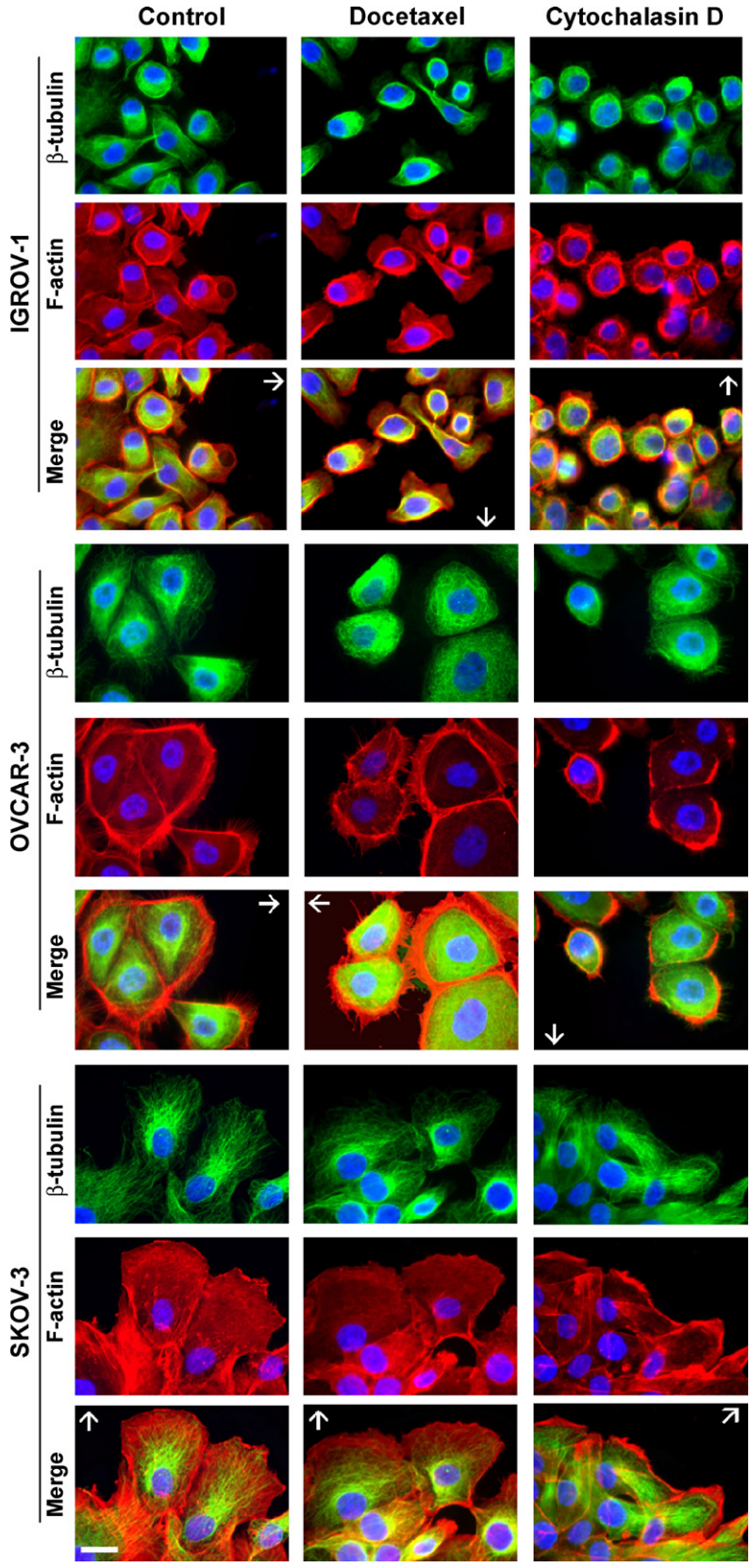

Fig. 5 – Effects of docetaxel and cytochalasin D on the structure of the tubulin and actin cytoskeleton of human ovarian cancer cells. β-Tubulin (green), F-actin (red) and nuclear (blue) staining of IGROV-1, OVCAR-3 and SKOV-3 is shown after they had grown to confluence, were treated or not with drugs (IC50 values as depicted in Table 2) for 1 h, wounded with a pipette tip and allowed to migrate for 8 h. The arrows point towards the direction of supposed cell movement. Bar = 10 μm. The images are representative for one out of three independent experiments.

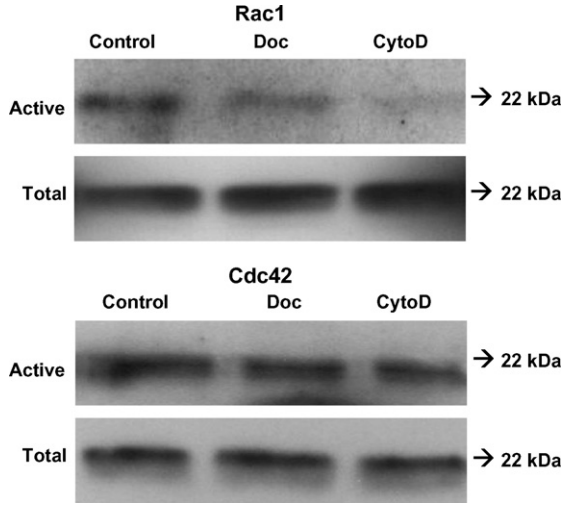

Fig. 6 – Effects of docetaxel and cytochalasin D on the activity of Rac1 and Cdc42 in OVCAR-3. Semi-confluent cells in minimal medium were stimulated by adding complete culture medium in the presence or absence of drugs (IC50, values in Table 2) for 1 h. The signal for active Rac1/Cdc42 was obtained by capturing the chemoluminescence reaction for 30 min, while total Rac1/Cdc42 was obtained after a 15 min exposure time. The experiments were carried out three times and yielded comparable results. Doc, docetaxel; CytD, cytochalasin D.

As expected, control cytotoxic agents cisplatin and doxorubicin did not significantly affect motility. Cytochalasin D was clearly more potent than docetaxel, epothilone B and vinblastine in inhibiting migration and invasion OVCAR-3, SKOV-3 and IGROV-1. Interference with microtubule dynamics by docetaxel at 50% growth-inhibiting concentrations only slightly altered the structure of the tubulin cytoskeleton. The activity of Rac1/Cdc42 in OVCAR-3 cells was reduced to a minor extent. In contrast, hindrance of actin dynamics by cytochalasin D at a dose inhibiting 50% of cell growth resulted in loss of lamellipodial extensions, the formation of thick layers of F-actin and disorder in cellular organization In OVCAR-3 cells this process was associated with a clear reduction in the activity of Rac1.

The properties of a panel of cytotoxic agents to prevent motility of cancer cells were investigated at subtoxic concentrations (HNTC) and at IC50 for an incubation period of 1 h. Each individual experiment was monitored with a parallel MTT assay to reassure that the drug concentrations used were representative for HNTC or IC50. Drug exposure periods of 1 h were selected because most cytotoxic agents given to cancer patients are either administered as bolus injections or infusions of short duration. All concentrations of the drugs that we calculated were well below the peak plasma levels that can generally be reached in patients, except for cisplatin. The IC50 values of cisplatin slightly exceeded the maximum plasma concentration of approximately 14 μM of intact cisplatin that can be reached after a 1-h infusion of 75 mg/m^2 in patients [15]. The maximum concentrations in patients are for doxorubicin given as a bolus injection of 60 mg/m^2 approximately 1 μM [16], for docetaxel 75–100 mg/m^2 given for 1 h approximately 4 μM [17] and for vinblastine 7–10.8 mg/m^2 given as a bolus injection approximately 160 nM [18]. No clinical data are available on cytochalasin D and peak plasma levels of epothilone B have yet to be reported.

Earlier studies have already indicated the potential use of cytoskeleton-targeting agents in the evasion of metastasis formation. *In vitro*, paclitaxel has been shown to inhibit human ovarian cancer cell migration, among which was SKOV-3, in a 4-h chemotaxis experiment at concentrations not inhibiting proliferation [19]. Paclitaxel was also able to inhibit OVCAR-3 invasion and migration after a 6-h incubation period at concentrations not affecting cell viability [20]. *In vivo*, docetaxel was shown to have antimetastatic properties in a SCID-mouse model of human prostate cancer bone metastases [21]. Although hardly effective by itself, combination of docetaxel with the angiogenesis inhibitor TNP-470 completely abolished lymph node metastasis formation of orthotopically implanted human transitional cell carcinoma in the bladder of nude mice [22]. Vinca family members conophylline and vinorelbine, both at non-cytotoxic concentrations for exposure times of 24–48 h, have been identified for their anti-invasive properties in, respectively, human endometrial cancer cells and human transitional cell bladder carcinoma cells [23,24]. Under the *in vitro* conditions using non-toxic or 50% growth-inhibiting concentrations in our experiments we did not find microtubule-targeting agents to have high potency to obstruct cancer cell motility, which is in contrast to our previous findings in endothelial cells [9]. We might, however, observe inhibition of ovarian cancer cell motility upon longer drug exposure periods of these compounds, since *in vitro* experiments mentioned above applied drugs for a period considerably longer than 1 h [19,20,23,24]. In addition, *in vivo* administration of docetaxel was carried out repeatedly to prevent the formation of metastases [21,22]. Our results obtained with cytochalasin D are in line with previous observations that this compound at a non-toxic concentration inhibited motility of a human melanoma cell line [25] and migration of a human non-small cell lung cancer and breast cancer cell line [26], although in both assays exposure times were longer than the 1 h we have applied.

Experiments revealing the structure of the microtubule and actin cytoskeleton (Fig. 5) support the premise that the actin cytoskeleton is in charge of ovarian cancer cell motility. The Rho GTPase family member Rac1 is known to stimulate the formation of actin extensions in the direction of cell movement. It is activated via microtubule plus end growth in the leading edge of migrating cells. This microtubule growth is induced after actin-associated microtubules buckle and break as a result of retrograde flow of polymerizing actin cables [27]. Obstruction of actin polymerization will, therefore, likely result in decreased Rac1 activity. While in OVCAR-3 cells stabilization of microtubules by docetaxel only slightly inhibited Rac1 activity, we indeed found clearly reduced Rac1 activity after interference with actin polymerization by cytochalasin D (Fig. 6). Inhibition of Rac1 activity after treatment with taxanes has already been established [9,28,29], but it now appears that cytochalasin D is more efficient in the inhibition of Rac1 function.

Cdc42, also a Rho GTPase family member, mediates cell polarization because of which migration is initiated in the correct direction [8,30]. The chaotic morphology upon cytocha-

lasin D treatment might be the result of disturbed polarization as a consequence of reduced Cdc42 activity. Cdc42 activity, however, was not clearly affected by docetaxel or cytochalasin D in OVCAR-3 cells. Cdc42 activation and actin polymerization function in a positive feedback loop. Yet, it has been proposed that initial Cdc42 activation occurs by an actin-independent mechanism, while for maintenance of Cdc42 polarization a correct orientation of actin cables is required [31].

For tumor cell metastasis formation there appear to be at least three necessary stages of cellular function: adherence to an extracellular matrix, release of proteolytic enzymes, and the motile response itself. Two out of our five cell lines lacked spontaneous motility as visualized in the wound assay. It has been demonstrated in human squamous cell carcinoma cell lines that epidermal growth factor receptor (EGFR) is required for invasion stimulated by EGF, since keratinocytes expressing low levels of EGFR do not invade [32]. In addition, HER2 expression in human breast cancer cell lines facilitated invasion upon stimulation with EGF-related peptides [33]. Of interest, spontaneous migration under 10% FCS conditions was only apparent in our ovarian cancer cell lines expressing EGFR, since EGFR is virtually absent in the non-motile cell lines A2780 and H134 (data not shown). It remains to be determined in ovarian cancer, whether EGFR signaling is involved in the motile response.

In conclusion, interference with actin dynamics is more efficient in the inhibition of human ovarian cancer cell motility than disturbance of microtubule function. Therefore, the actin cytoskeleton should be considered as a therapeutic target to prevent metastasis formation [34]. Actin-interfering agents are not specific for cancer cells. Since Rho GTPases, such as Rac1, are overexpressed in a variety of tumors, these may be attractive for drug development [7]. Design of small molecule inhibitors targeting Rac1 is underway [35]. Such compounds might particularly be useful in patients with no or minimal residual disease after optimal debulking surgery in order to improve the cure rate in ovarian cancer.

Conflict of interest statement

None declared.

Acknowledgments

Financial support: This work was partially funded by an unrestricted grant of sanofi aventis. GPvNA was supported by The Netherlands Heart Foundation (The Hague, grant 2003T032).

REFERENCES

[1] Nickles Fader A, Rose PG. Role of surgery in ovarian carcinoma. J Clin Oncol 2007;25:2873–83.
[2] Naora H, Montell DJ. Ovarian cancer metastasis: integrating insights from disparate model organisms. Nat Rev Cancer 2005;5:355–66.
[3] Waterman-Storer CM, Salmon E. Positive feedback interactions between microtubule and actin dynamics during cell motility. Curr Opin Cell Biol 1999;11:61–7.
[4] Etienne-Manneville S. Actin and microtubules in cell motility: which one is in control? Traffic 2004;5:470–7.
[5] Ridley AJ. Rho GTPases and cell migration. J Cell Sci 2001;114:2713–22.
[6] Raftopoulou M, Hall A. Cell migration: Rho GTPases lead the way. Dev Biol 2004;265:23–32.
[7] Vega FM, Ridley AJ. Rho GTPases in cancer biology. FEBS Lett 2008;582:2093–101.
[8] Cau J, Hall A. Cdc42 controls the polarity of the actin and microtubule cytoskeletons through two distinct signal transduction pathways. J Cell Sci 2005;118:2579–87.
[9] Bijman MN, Van Nieuw Amerongen GP, Laurens N, Van Hinsbergh V, Boven E. Microtubule-targeting agents inhibit angiogenesis at subtoxic concentrations, a process associated with inhibition of Rac1 and Cdc42 activity and changes in the endothelial cytoskeleton. Mol Cancer Ther 2006;5:2348–57.
[10] Jordan MA, Wilson L. Microtubules and actin filaments: dynamic targets for cancer chemotherapy. Curr Opin Cell Biol 1998;10:123–30.
[11] Goodin S, Kane MP, Rubin EH. Epothilones: mechanism of action and biologic activity. J Clin Oncol 2004;22:2015–25.
[12] Ponti A, Machacek M, Gupton SL, Waterman-Storer CM, Danuser G. Two distinct actin networks drive the protrusion of migrating cells. Science 2004;305:1782–6.
[13] Buick RN, Pullano R, Trent JM. Comparative properties of five human ovarian adenocarcinoma cell lines. Cancer Res 1985;45:3668–76.
[14] Kolfschoten GM, Hulscher TM, Duyndam MC, Pinedo HM, Boven E. Variation in the kinetics of caspase-3 activation. Bcl-2 phosphorylation and apoptotic morphology in unselected human ovarian cancer cell lines as a response to docetaxel. Biochem Pharmacol 2002;63:733–43.
[15] Verschraagen M, Boven E, Ruijter R, Van der Born K, Berkhof J, Hausheer FH, et al. Pharmacokinetics and preliminary clinical data of the novel chemoprotectant BNP7787 and cisplatin and their metabolites. Clin Pharmacol Ther 2003;74:157–69.
[16] Brenner DE, Grosh WW, Noone R, Stein R, Greco FA, Hande KR. Human plasma pharmacokinetics of doxorubicin: comparison of bolus and infusional administration. Cancer Treat Symp 1984;3:77–83.
[17] Bruno R, Hille D, Riva A, Vivier N, Bokkel Huinink WW, van Oosterom AT, et al. Population pharmacokinetics/pharmacodynamics of docetaxel in phase II studies in patients with cancer. J Clin Oncol 1998;16:187–96.
[18] Nelson RL, Dyke RW, Root MA. Comparative pharmacokinetics of vindesine, vincristine and vinblastine in patients with cancer. Cancer Treat Rev 1980;7 (Suppl 1):17–24.
[19] Belotti D, Rieppi M, Nicoletti MI, Casazza AM, Fojo T, Taraboletti G, et al. Paclitaxel (Taxol®) inhibits motility of paclitaxel-resistant human ovarian carcinoma cells. Clin Cancer Res 1996;2:1725–30.
[20] Westerlund A, Hujanen E, Höyhtyä M, Puistola U, Turpeenniemi-Hujanen T. Ovarian cancer cell invasion is inhibited by paclitaxel. Clin Exp Metastasis 1997;15: 318–28.
[21] Li Y, Kucuk O, Hussain M, Abrams J, Cher ML, Sarkar FH. Antitumor and antimetastatic activities of docetaxel are enhanced by genistein through regulation of osteoprotegerin/receptor activator of nuclear factor-κB (RANK)/RANK ligand/MMP-9 signaling in prostate cancer. Cancer Res 2006;66:4816–25.
[22] Inoue K, Chikazawa M, Fukata S, Yoshikawa C, Shuin T. Docetaxel enhances the therapeutic effect of the

angiogenesis inhibitor TNP-470 (AGM-1470) in metastatic human transitional cell carcinoma. Clin Cancer Res 2003;9:886–99.
[23] Irie T, Kubushiro K, Suzuki K, Tsukazaki K, Umezawa K, Nozawa S. Inhibition of attachment and chemotactic invasion of uterine endometrial cancer cells by a new vinca alkaloid, conophylline. Anticancer Res 1999;19: 3061–6.
[24] Bonfil RD, Russo DM, Schmilovich AJ. Exposure to vinorelbine inhibits in vitro proliferation and invasiveness of transitional cell bladder carcinoma. J Urol 1996;156: 517–21.
[25] Stracke ML, Soroush M, Liotta LA, Schiffmann E. Cytoskeletal agents inhibit motility and adherence of human tumor cells. Kidney Int 1993;43:151–7.
[26] Hayot C, Debeir O, Van Ham P, Van Damme M, Kiss R, Decaestecker C. Characterization of the activities of actin-affecting drugs on tumor cell migration. Toxicol Appl Pharmacol 2006;211:30–40.
[27] Wittmann T, Waterman-Storer CM. Cell motility: can Rho GTPases and microtubules point the way? J Cell Sci 2001;114:3795–803.
[28] Waterman-Storer CM, Worthylake RA, Liu BP, Burridge K, Salmon ED. Microtubule growth activates Rac1 to promote lamellipodial protrusion in fibroblasts. Nat Cell Biol 1999;1:45–50.
[29] Hu YL, Li S, Miao H, Tsou TC, Del Pozo MA, Chien S. Roles of microtubule dynamics and small GTPase Rac in endothelial cell migration and lamellipodium formation under flow. J Vasc Res 2002;39:465–76.
[30] Etienne-Manneville S, Hall A. Rho GTPases in cell biology. Nature 2002;420:629–35.
[31] Irazoqui JE, Howell AS, Theesfeld CL, Lew DJ. Opposing roles for actin in Cdc42p polarization. Mol Biol Cell 2005;16:1296–304.
[32] Malliri A, Symons M, Hennigan RF, Hurlstone AF, Lamb RF, Wheeler T, et al. The transcription factor AP-1 is required for EGF-induced activation of rho-like GTPases, cytoskeletal rearrangements, motility, and in vitro invasion of A431 cells. J Cell Biol 1998;143: 1087–99.
[33] Spencer KS, Graus-Porta D, Leng J, Hynes NE, Klemke RL. ErbB2 is necessary for induction of carcinoma cell invasion by ErbB family receptor tyrosine kinases. J Cell Biol 2000;148:385–97.
[34] Giganti A, Friederich E. The actin cytoskeleton as a therapeutic target: state of the art and future directions. Prog Cell Cycle Res 2003;5:511–25.
[35] Nassar N, Cancelas J, Zheng J, Williams DA, Zheng Y. Structure-function based design of small molecule inhibitors targeting Rho family GTPases. Curr Top Med Chem 2006;6:1109–16.